Journal of Molecular Graphics and Modelling 38 (2012) 455–464

Contents lists available at SciVerse ScienceDirect

Journal of Molecular Graphics and Modelling

journal homepage: www.elsevier.com/locate/JMGM

The Wolf method applied to the type I methane and carbon dioxide gas hydrates

Alireza Sadeghifar[a], Mitra Dadvar[a,*], Safoora Karimi[a], Ahmadreza F. Ghobadi[b]

[a] Department of Chemical Engineering, Amirkabir University of Technology (Tehran Polytechnic), Tehran 15875-4413, Iran
[b] Department of Chemical and Biomolecular Engineering, University of Akron, Akron, OH 44325, USA

ARTICLE INFO

Article history:
Accepted 5 October 2012
Available online 13 October 2012

Keywords:
Gas hydrate
Monte Carlo simulation
Electrostatic interactions
The Wolf method
Structural properties

ABSTRACT

The Wolf method [42] is introduced to handle long-range electrostatic interactions as a viable alternative to the most common methods, i.e., the Ewald Sum and its modifications (PPPM, PME and SPME), the Reaction Field method, and the Lekner technique for predicting the structure of type I clathrate hydrates. In comparison with the Ewald Sum family, it is computationally more time-saving and mathematically much simpler. It is also physically more meaningful than the Ewald Sum for disordered systems, liquids and crystals. In comparison with the Reaction Field method, it does not require the calculation of the dielectric constant during the simulation. The computational cost of the Wolf method is also much less than the Lekner method. *NPT* and *NVT* ensemble Monte Carlo simulations are performed to calculate energetic and structural properties of CH_4 and CO_2 gas hydrates at formation pressures and temperatures. The optimum values of the control parameters employed in the Wolf method are evaluated and the criteria used for the calculations are discussed. Finally, the results are compared with several simulation results and experimental data and satisfactory agreement is achieved.

1. Introduction

Clathrate hydrates are non-stoichiometric ice-like crystalline compounds comprised of water molecules which form the host lattice, and some guest molecules trapped in the cages of the hydrogen-bonded water lattice [1–8]. The empty hydrate is not stable and it has not been observed in nature yet [9–11]. However, if a second component such as methane or other light hydrocarbons is included in its structure, it can be stabilized [9,10]. Owing to the important applications of natural gas hydrates, the interest to understand and quantify its properties has increased [9]. Thus, molecular-based theories and molecular simulations have been one of the main and growing areas of scientific development over the past decades [12–20]. Since water molecules exist in the hydrate lattice, for an exact description of the system, the strong electrostatic interactions have to be included [21,22]. One of the technical problems in molecular simulations is the correct modeling of the long-range electrostatic interactions. The Ewald Sum (henceforth referred to as ES) method [23,24] is the most common method to deal with electrostatic interactions in hydrate simulations [22,25–41]. Although the aforementioned method is exact, its Fourier part is time-consuming [42,43]. Therefore, effective methods such as Particle–Particle–Particle-Mesh (PPPM) [23,44–46], Smooth Particle Mesh Ewald (SPME) [47–49] and Particle Mesh Ewald (PME) [50–52] are used in hydrate simulations to overcome this difficulty [19,53–61]. These methods utilize fast Fourier transform to optimize the Fourier part and speed up the calculations [43,62]. Another problem of the ES method is the assumption behind it, i.e., the periodicity of the system. The inherent periodicity may cause possible artifacts and hence its application to disordered systems (such as melts, free surfaces and interfaces) and liquids has long been questionable [62–64]. In addition, the reciprocal space term in the ES method is implemented over replicated cells [65], which are not spherically symmetrical. Since the Coulomb (electrostatic) interaction shows spherical symmetry, the physics of the ES method is problematic for disordered systems and crystals [63].

The other method used in the hydrate simulations [21] is the Reaction Field (henceforth referred to as RF) method [66,67]. The RF method is simple and computationally efficient, but its main restriction is the need for the dielectric constant of the surrounding media which is unknown under some conditions and should be calculated in a self-consistent way [66,68–70], making the method inefficient. Moreover, in this method the medium over the cutoff radius is assumed to be a continuous fluid, which is likely to be reasonable for homogeneous fluids [23,62,66,71].

There are also some other alternatives to calculate the electrostatic interactions in hydrate simulations [72–76] such as the Lekner method [77]. The serious drawback of this technique is its computational time, although it does not involve any adjustable parameters or assumptions concerning neutralizing charge distributions like those in the ES method [72,78].

* Corresponding author. Tel.: +98 21 6454 3173; fax: +98 21 6640 5847.
E-mail addresses: alirezasadeghifar@gmail.com (A. Sadeghifar), dadvar@aut.ac.ir (M. Dadvar).

1093-3263/$ – see front matter © 2012 Elsevier Inc. All rights reserved.
http://dx.doi.org/10.1016/j.jmgm.2012.10.002

Nomenclature

N	total number of ions
q	charge of the ion (C)
r	distance between ions (Å)
E	total energy (J)
α	damping parameter ($Å^{-1}$)
R_C	cut-off radius (Å)
L	length of simulation box (Å)
σ	collision diameter (Å)
κ	damping parameter in real space ($Å^{-1}$)
k	number of wave vectors in reciprocal space
ε	depth of the potential well (J)
k_B	Boltzmann constant (J/K)
l	bond length (Å)
T	temperature (K)
P	pressure (Pa)
U	configurational energy (kcal/mol)
ε_0	relative permittivity ($C^2/(J Å)$)

Superscript

Mad	abbreviation for Madelung

Subscript

O	oxygen
H	hydrogen
M	methane
w	water
u	guest
tot	abbreviation for total
Box	simulation box
C	cut-off
B	Boltzmann

Another appropriate method to deal with long-range electrostatic interactions has been developed by Wolf et al. [42]. The method is based on the evidence that the Coulomb potential in condensed systems is short-ranged rather than long-ranged. In their three-step procedure, they developed a new expression for calculating electrostatic (Coulomb) interactions [42]. Their final equation is more convenient to use [64] and has the main advantages such as requiring no experimental data and having lower computational cost [63,64,70].

Demontis et al. [63] employed the original form of the Wolf method in the simulation of liquid water. They optimized the necessary parameters for the new method and obtained good results with significantly faster simulations than those using the ES method. The method is also utilized in other researches [70,71,79–87]. Zahn et al. [88] employed a slightly modified form of the Wolf method to calculate the static properties of liquid water and discussed a two-step procedure to calculate the necessary parameters of their final equation. Kast et al. [89], Ribeiro [90] and Hansen et al. [91] applied Zahn's equation to various materials. Fennell and Gezelter [62] extended the Wolf equation and reproduced energetic and dynamic characteristics of ionic fluids, water, and ionic solutions obtained from the SPME method. Their final equation was used in different molecular simulation studies [43,92,93].

The present study aims at testing the validity of the original form of the Wolf method in calculating the properties of type I gas hydrates, instead of using the ES technique and its three alterations (PPPM, PME and SPME), the RF and Lekner methods. Thus, the rest of the article is organized as follows. In Section 2, the theory of the Wolf method is explained briefly along with its advantages compared to the previous electrostatic techniques. The details of the simulations and the strategy used for computing the parameters employed in the Wolf method are explained in Section 3. In Section 4, the calculated properties are presented where they are compared with the results of previous simulations and experimental data. The conclusions are summarized in the final section.

2. Theory

The total electrostatic interaction for a system of N ions is given by [71]

$$E_{tot} = \frac{1}{2}\sum_{i=1}^{N}\sum_{j\neq i=1}^{N}\frac{q_i q_j}{4\pi\varepsilon_0 r_{ij}} \tag{1}$$

where q_i is the charge of the ion i and r_{ij} is the distance between ions i and j. Eq. (1) is a conditionally convergent summation being well-known as Madelung problem [69,94]. The earliest solution to this problem was proposed by Ewald [95] which has been used extensively in the molecular simulations of ionic liquids and crystals [42,63]. However, the Ewald method is slow where its computational time scales as $O(N^2)$ for a system of N charges. A reciprocal and real space cutoff optimization provides only a slight improvement by reducing the computational time to an order of $O(N^{3/2})$ [23,24,42,49,51,62,96–99]. Therefore, for large systems (large N) this method becomes prohibitively expensive [24].

To overcome this difficulty, three mesh implementations of the ES method, which are similar in spirit but different in details, have been proposed for calculating the long-range electrostatic interactions in molecular simulations. These methods are the original Particle–Particle Particle-Mesh (PPPM) method of Hockney and Eastwood [44], the Particle Mesh Ewald (PME) method of Darden et al. [50], and an approach by Essmann et al. [47] which is usually referred to as the Smooth Particle Mesh Ewald (SPME) method. These methods apply the fast Fourier transforms to compute the reciprocal-space term and reduce the computational load of the traditional ES method from $O(N^2)$ to $O(N \log N)$ [24,45,48,49,51,62,71,100,101].

Another alternate to solve Eq. (1) is the Onsager's Reaction Field (RF) method [67], which is much easier to implement than the ES method and its modifications [23,71]. Also, it has a relatively fast algorithm where the computational time scales as O(N) [23], however, its main restriction is the need for the dielectric constant of the surrounding media, making the method inefficient [23,66].

There is also another formulation to treat long-range electrostatic interactions called the Lekner method, proposed by Lekner [77], which offers an exact mathematical solution to the problem. This method takes the summation of the Coulomb interactions entirely in the reciprocal space [78] causing the computational cost to scale as $O(N^2)$ [77,102–104] and, as it was noted previously, this is the main downside of the method.

Wolf et al. [42] solved Eq. (1) in three steps by introducing a charge-neutralized damped potential. Their final equation is in the following form:

$$E_{tot}^{Mad}(R_C) \approx \frac{1}{2}\sum_{i=1}^{N}\sum_{\substack{j\neq i\\(r_{ij}<R_C)}}\frac{1}{4\pi\varepsilon_0}\left(\frac{q_i q_j erfc(\alpha r_{ij})}{r_{ij}} - \frac{q_i q_j erfc(\alpha R_C)}{R_C}\right) - \left(\frac{erfc(\alpha R_C)}{2R_C} + \frac{\alpha}{\pi^{1/2}}\right)\sum_{i=1}^{N}\frac{q_i^2}{4\pi\varepsilon_0} \tag{2}$$

where $E_{tot}^{Mad}(R_C)$ is the Madelung energy, R_C is the cut off radius, *erfc* is the complementary error function and α is the damping parameter. Since this equation only requires evaluating of a

Table 1
Computational time of methods of treating long-range electrostatic interactions as a function of the number of charged particles in the simulation box (N).

Method	Author(s) (year)	Computational cost (time)
Ewald	Ewald (1921)	$O(N^{3/2})$
Reaction Field	Lars Onsager (1936)	O(N)
PPPM	Hockney and Eastwood (1988)	O(N log N)
Lekner	Lekner (1991)	$O(N^2)$
PME	Darden et al. (1993)	O(N log N)
SPME	Essmann et al. (1995)	O(N log N)
Wolf	Wolf et al. (1999)	O(N)

pairwise sum truncated in an appropriate distance, the computational cost scales linearly with increasing system size (N), i.e., it is of order O(N) [42,62,70,82,85,93,104].

In comparison with the ES final equation [23,24] and its modifications [44,47,50], the new equation does not have the Fourier part, which is the most time-consuming part in treating long-range interactions [70,105,106]. It also consists of only a direct pair summation over the distances with constant terms, making it mathematically much simpler. In addition, since the new method lacks the added periodicity in the ES procedure, it does not have the subsequent possible artifacts [43,62]. Furthermore, by retaining the spherical symmetry of the Coulomb potential, the Wolf method is physically more suitable for liquids and crystals than the ES method [63]. Moreover there are only two control parameters in the Wolf equation (α and R_C), which makes the simulation more convenient, whereas the number of control parameters in the ES method is three (κ, R_C and k-vectors) [106].

Furthermore, the Wolf method does not require the prior knowledge about the dielectric constant as in the case of the RF method. There is also no similar restriction on using the method properly for homogeneous fluids. Finally, as it was pointed out, the Wolf approach has a linear scaling with system size (N), while the Lekner technique is of order of a higher power of N ($O(N^2)$), so the former is clearly faster. Therefore, the application of the Wolf method for more complex systems is preferred not only for being computationally time-saving but also for its simplicity. In Table 1, the computational time of these methods as a function of the number of charged species (N) in the simulation box is summarized.

3. Methods

3.1. Simulation details

The simulated systems are fully occupied type I methane and carbon dioxide clathrate hydrates. *NPT* and *NVT* ensemble Monte Carlo (MC) computer simulations are performed at formation pressures and temperatures. The cubic simulation box consists of $2 \times 2 \times 2$ replicas of the unit cell of type sI clathrate hydrate with the initial edge size of 24.06 Å. Each unit cell is 12.03 Å long and contains 46 water molecules with 8 guest molecules encaged in each cavity. Periodic boundary conditions are applied for all three Cartesian directions. For both the rigid and flexible *NVT* and *NPT* runs, the starting configurations, i.e., the locations of the water oxygen and hydrogen atoms and the center of mass of the guest molecules, are taken from a previous study [107], which was based on the crystallography of ethylene oxide hydrate at −25 °C [108]. All the simulations are carried out for a total number of 9×10^5 cycles where the initial 3×10^5 steps are used for equilibration and the subsequent period (production run in which averages are calculated) is conducted in order to predict the static properties. The standard deviations of the energies are estimated by dividing the production run into six segments of length 1×10^5 steps, according to the standard approach [66]. To model the host–host interactions, the SPC [109], SPC/E [110] and TIP4P [111] potential models of water are used with the parameters given in Table 2. These models incorporate a Lennard–Jones potential for the oxygen–oxygen interactions and a Coulomb one for the electrostatic interactions between each pair of charged sites. The water molecule is assumed to be rigid and hence all the bond lengths and the bond angles of the individual molecules are kept fixed during the MC simulation.

Table 2
Intermolecular potential parameters for the different water models.

Model	ε_{O-O}/k_B (K)	σ_{O-O} (Å)	q_H	l_{O-M} (Å)	l_{O-H} (Å)	∠HOH (°)
SPC	78.23	3.16600	0.4100	–	1.0000	109.47
SPC/E	78.23	3.16600	0.4238	–	1.0000	109.47
TIP4P	77.99	3.15365	0.5200	0.15	0.9572	104.52

Long-range electrostatic interactions are handled by the Wolf method. The computation of the parameters, which are needed in the wolf equation, will be discussed in Section 3.2. Guest molecules are treated as spherical particles and the short-range intermolecular van der Waals interactions among guest–guest and guest–host sites are calculated using Lennard–Jones (LJ) 12-6 potential model. The guest–guest LJ interaction parameters are listed in Table 3. The cross LJ interaction parameters are evaluated by adopting Lorentz–Berthelot combining rules [38,39,112,113]. The cut off radii for LJ and Coulomb interactions are taken the same and long-range dispersion corrections are applied to the energy for the truncation of the LJ potential.

3.2. Optimization of the parameters

The first step in the simulations using the Wolf method is to characterize the optimum values of the parameters required in the final equation (Eq. (2)). Despite the different strategies used in the previous simulations [43,63,70,88], this work is based on a new technique to optimize the required parameters. The new approach considers the different types of energies involved in the total energy of the hydrates.

In order to determine the optimum values of the parameters, a system of fully occupied methane hydrate is chosen (the results for the other type I gas hydrate, i.e., CO_2 hydrate, follow the same functional form as well). *NPT* ensemble Monte Carlo simulations were run at 270 K and 5 MPa by using the Wolf method for calculating the electrostatic interactions. Fig. 1 shows the total configurational internal energies (per total particles) of the system for the RF and the Wolf method, in which the latter is a function of damping constant and cut off distance.

According to Fig. 1 at a given R_C, the deviation from the reference energy (dashed line) first decreases and then increases with the increase in αL. In other words, the deviation is more for large and small damping constants in the given cut off radius. It is also evident that for a smaller value of R_C, larger amount of damping parameter is needed. In fact, one can speed up the computations by applying a smaller R_C, but a larger amount of α, which inevitably results in a larger systematic error, is required to ensure convergence [42,63,64]. Consequently, an appropriate combination of the

Table 3
Intermolecular potential parameters for the Lennard–Jones guest molecules [20].

Model	ε/k_B (K)	σ (Å)
CO_2	232.0	3.643
CH_4	148.0	3.73

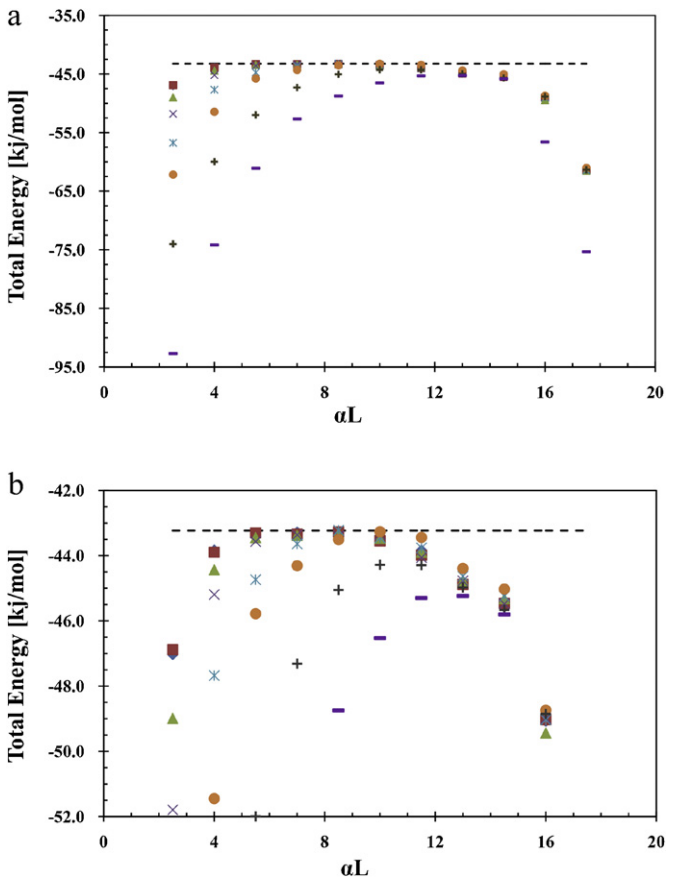

Fig. 1. Total internal energies (per total particles) for methane hydrate at 270 K and 5 MPa obtained from the RF method [Ref. [20]] (dashed line) together with the energies obtained from the Wolf method as a function of R_C/L_{Box} and α (◆: $R_C/L_{Box}=0.50$, ■: $R_C/L_{Box}=0.45$, ▲: $R_C/L_{Box}=0.40$, ✕: $R_C/L_{Box}=0.35$, ✳: $R_C/L_{Box}=0.30$, ●: $R_C/L_{Box}=0.25$, ✚: $R_C/L_{Box}=0.20$ and ▬: $R_C/L_{Box}=0.15$). Figure (b) is a magnified picture of figure (a).

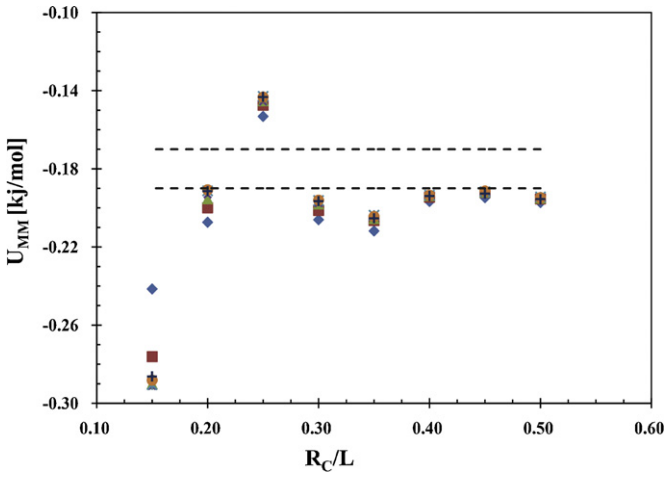

Fig. 2. Comparison of the methane–methane internal energies (per water molecule) at 270 K and 5 MPa obtained from the Wolf method for different values of R_C/L_{Box} and α (◆: $\alpha L_{Box}=2.5$, ■: $\alpha L_{Box}=4.0$, ▲: $\alpha L_{Box}=5.5$, ✕: $\alpha L_{Box}=7.0$, ✳: $\alpha L_{Box}=8.5$, ●: $\alpha L_{Box}=10.0$ and ✚: $\alpha L_{Box}=11.5$) with the methane–methane energy estimated by the RF method in Ref. [20]. The two dashed lines show the upper and lower limit of the energy deviation obtained from the RF method.

parameters should be found to reduce the computational effort and damping error simultaneously.

Referring again to Fig. 1, the best values for α, which result in the minimum error between Wolf and RF methods, are obtained for $0.2 \le (R_C/L_{Box}) \le 0.5$, where L_{Box} is the simulation side length. Considering the desired damping constants, it is viewed that for small quantities of R_C, the range of the proper damping constants drops noticeably. For example, for $R_C/L_{Box}=0.5$, the appropriate range is from $\alpha=4/L_{Box}\approx 0.17$ to $\alpha=11.5/L_{Box}\approx 0.48$, while for $R_C/L_{Box}=0.25$ the suitable quantities of α are between 0.35 and 0.48. It is also obvious that the decline in the energies for increasing α is almost independent of R_C, especially for $0.2 \le (R_C/L_{Box}) \le 0.5$. This result is very close to the result of Demontis et al. [63].

Demontis et al. [63] derived criteria to calculate optimum values of the parameters needed in the Wolf final equation and found that if $R_C \le (L_{Box}/2)$, the best values for the damping parameter are given by $\alpha R_C = 2$. They also analyzed the results of Wolf et al. [42] for MgO and NaCl, and found that satisfactory values for the Wolf parameters are achieved when $\alpha R_C \approx 2.3$. Referring to Fig. 1, it is observed that the present optimal results almost follow the mentioned rules concluded by Demontis et al. [63].

In Section 3.1, it was assumed that the cut off radii for LJ and Coulomb interactions are aequal. However, we have only considered the effect of the electrostatic interactions on cut off radius (see Fig. 1). In order to include the influence of the LJ interactions on R_C, the methane–methane internal energies which are obtained herein are compared, in Fig. 2, with those of Chialvo et al. [21] at the same pressure and temperature.

In order to simplify the discussion, only some valuable data are plotted in Fig. 2. In fact, U_{MM} (where M denotes methane and U is the internal energy) is the best choice to study the impact of LJ cut off radius on the resulting energies. This can be attributed to the fact that methane–methane interactions only consist of LJ interactions, which depend on R_C (not α).

According to Fig. 2, the value of R_C for which the methane–methane potential energies become constant is equal to $0.4L_{Box}$ and for larger quantities of R_C ($R_C \ge 0.4L_{Box}$) the amounts of U_{MM} converge to the correct value. As expected on the basis of LJ interactions' behavior, the converged energies are independent of α. Thus, in order to obtain correct LJ interactions, the cut off distance should satisfy the condition $R_C \ge 0.4L_{Box}$. Assuming $L_{Box} \approx 24.0$ Å, the best results for R_C should follow the rule $R_C \ge 2.58\sigma_{MM}$, where M indicates methane and σ is the molecular diameter. Since $\sigma_{MM(CO_2)} < \sigma_{MM(CH_4)}$ (see Table 3), the same rule is almost applicable to the carbon dioxide as well.

4. Results and discussion

To evaluate the energetic and structural results, the cut off radius and the damping parameter are set equal to $0.4L_{Box}$ and $5.5/L_{Box}$, respectively. The choice of the parameters is based on the discussions in Section 3.2.

4.1. Energetic results

In Tables 4–6, the average potential energies (per total particles) calculated from the *NVT* and *NPT* ensemble MC simulations with different electrostatic and water potential models are reported, together with the earlier estimated results obtained from almost the same water potential models and under the same conditions. The standard deviations showing the precision of the results are also presented in the tables. In all of the tables, subscripts w and u denote water and methane (or carbon dioxide), respectively. It should also be noted that the methane and carbon dioxide models used in this research are exactly the same as those applied in the studies by Førrisdahl et al. [28] and Chialvo et al. [21], though they are different from the models used in other simulations in Tables 4–6.

Table 4
NVT ensemble simulation results for CH_4 hydrate.

Electrostatic model	T (K)	Water model	$-U_{tot}$ (kcal/mol)	$-U_{ww}$ (kcal/mol)	$-U_{wu}$ (kcal/mol)	$-U_{uu}$ (kcal/mol)
Ewald[a]	50	AMOEBA	11.80	–	–	–
		COS/G2	11.85	–	–	–
	125	AMOEBA	11.37	–	–	–
		COS/G2	11.42	–	–	–
	200	AMOEBA	10.91	–	–	–
Ewald[b]	270	SPC	10.26 ± 0.11	9.660 ± 0.1	0.568 ± 0.008	0.0346 ± 0.002
Lekner[c]	50	SPC	11.48 ± 0.02	10.85 ± 0.02	0.600 ± 0.01	0.0261 ± 0.002
		SPC/E	12.38 ± 0.02	11.75 ± 0.02	0.602 ± 0.01	0.0261 ± 0.002
		TIP4P	11.51 ± 0.02	10.89 ± 0.02	0.596 ± 0.01	0.0261 ± 0.002
	125	SPC	11.06 ± 0.02	10.46 ± 0.02	0.574 ± 0.01	0.0268 ± 0.002
		SPC/E	11.96 ± 0.02	11.36 ± 0.02	0.576 ± 0.01	0.0268 ± 0.002
		TIP4P	11.10 ± 0.02	10.50 ± 0.02	0.571 ± 0.01	0.0269 ± 0.002
	200	SPC	10.61 ± 0.02	10.03 ± 0.02	0.549 ± 0.01	0.0273 ± 0.002
		SPC/E	11.52 ± 0.02	10.94 ± 0.02	0.550 ± 0.01	0.0273 ± 0.002
		TIP4P	10.66 ± 0.02	10.08 ± 0.02	0.547 ± 0.01	0.0274 ± 0.002
Wolf[d]	50	SPC	11.71 ± 0.04	10.94 ± 0.03	0.648 ± 0.002	0.0364 ± 0.0001
		SPC/E	12.50 ± 0.07	11.89 ± 0.01	0.648 ± 0.002	0.0365 ± 0.0000
		TIP4P	11.74 ± 0.04	10.96 ± 0.07	0.643 ± 0.003	0.0365 ± 0.0001
	125	SPC	11.29 ± 0.06	10.59 ± 0.02	0.619 ± 0.002	0.0371 ± 0.0001
		SPC/E	12.09 ± 0.06	11.45 ± 0.03	0.621 ± 0.002	0.0371 ± 0.0001
		TIP4P	11.31 ± 0.04	10.66 ± 0.04	0.617 ± 0.002	0.0372 ± 0.0001
	200	SPC	10.77 ± 0.03	10.19 ± 0.03	0.593 ± 0.003	0.0375 ± 0.0000
		SPC/E	11.75 ± 0.03	11.11 ± 0.03	0.596 ± 0.003	0.0376 ± 0.0001
		TIP4P	10.79 ± 0.06	10.20 ± 0.03	0.592 ± 0.003	0.0376 ± 0.0001
	270	SPC	10.30 ± 0.03	9.700 ± 0.04	0.562 ± 0.003	0.0377 ± 0.0001

[a] Jiang et al. [97].
[b] Førrisdahl et al. [27].
[c] English and McElroy [60].
[d] This work.

In the study by Jiang et al. [114], they validate their results, which were obtained from the ES method, by using the results calculated with the Lekner method in an earlier research [72]. Therefore; the Lekner results are superb references to test the validity of our results. From all the three tables it can be seen that under similar conditions, the results calculated from different electrostatic methods are almost indistinguishable from each other, confirming that the present energetic results are in very good agreement with the previously reported *NVT* and *NPT* simulation data [28,72,112,114].

According to Tables 4 and 5, it can be seen that at a given temperature, the internal energies computed by the Wolf method in the *NPT* ensemble are smaller than the corresponding ones in the *NVT* ensemble. This result is nearly identical to the previous result in the study by English and MacElroy [72]. In Table 4 at a definite

Table 5
NPT ensemble simulation results for CH_4 hydrate.

Electrostatic model	T (K)	P (MPa)	Water model	$-U_{tot}$ (kcal/mol)	$-U_{ww}$ (kcal/mol)	$-U_{wu}$ (kcal/mol)	$-U_{uu}$ (kcal/mol)
Ewald[a]	275	30	SPC/E	11.29 ± 0.03	–	–	–
Reaction Field[b]	270	5	SPC	10.32 ± 0.004	9.710 ± 0.01	0.579 ± 0.002	0.0366 ± 0.002
			SPC/E	10.52 ± 0.002	9.890 ± 0.01	0.608 ± 0.002	0.0406 ± 0.002
Lekner[c]	50	0.1	SPC	11.65 ± 0.02	10.98 ± 0.02	0.645 ± 0.01	0.0301 ± 0.002
			SPC/E	12.66 ± 0.02	11.97 ± 0.02	0.655 ± 0.01	0.0314 ± 0.002
			TIP4P	11.76 ± 0.02	11.08 ± 0.02	0.650 ± 0.01	0.0312 ± 0.002
	125	0.1	SPC	11.21 ± 0.02	10.58 ± 0.02	0.602 ± 0.01	0.0298 ± 0.002
			SPC/E	12.22 ± 0.02	11.58 ± 0.02	0.613 ± 0.01	0.0310 ± 0.002
			TIP4P	11.32 ± 0.02	10.68 ± 0.02	0.610 ± 0.01	0.0308 ± 0.002
	200	2	SPC	10.72 ± 0.02	10.13 ± 0.02	0.563 ± 0.01	0.0292 ± 0.002
			SPC/E	11.74 ± 0.02	11.13 ± 0.02	0.575 ± 0.01	0.0304 ± 0.002
Wolf[d]	275	30	SPC/E	11.37 ± 0.03	10.77 ± 0.02	0.577 ± 0.004	0.0409 ± 0.0000
	270	5	SPC	10.37 ± 0.02	9.77 ± 0.02	0.566 ± 0.004	0.0394 ± 0.0002
			SPC/E	11.39 ± 0.05	10.79 ± 0.03	0.580 ± 0.004	0.0409 ± 0.0001
	50	0.1	SPC	11.88 ± 0.04	11.15 ± 0.04	0.685 ± 0.003	0.0418 ± 0.0002
			SPC/E	12.89 ± 0.02	12.06 ± 0.05	0.699 ± 0.003	0.0434 ± 0.0002
			TIP4P	11.92 ± 0.04	11.28 ± 0.05	0.696 ± 0.002	0.0429 ± 0.0001
	125	0.1	SPC	11.36 ± 0.04	10.75 ± 0.04	0.646 ± 0.002	0.0412 ± 0.0001
			SPC/E	12.45 ± 0.03	11.75 ± 0.02	0.656 ± 0.003	0.0426 ± 0.0001
			TIP4P	11.49 ± 0.04	10.79 ± 0.04	0.653 ± 0.002	0.0423 ± 0.0002
	200	2	SPC	10.88 ± 0.03	10.23 ± 0.04	0.605 ± 0.003	0.0403 ± 0.0001
			SPC/E	11.91 ± 0.03	11.32 ± 0.03	0.615 ± 0.003	0.0419 ± 0.0000
			TIP4P	11.06 ± 0.02	10.37 ± 0.02	0.614 ± 0.003	0.0417 ± 0.0001

[a] Dornan et al. [95].
[b] Chialvo et al. [20].
[c] English and McElroy [60].
[d] This work.

Table 6
NPT ensemble simulation results for CO_2 hydrate.

Electrostatic model	T (K)	P (MPa)	Water model	$-U_{tot}$ (kcal/mol)	$-U_{ww}$ (kcal/mol)	$-U_{wu}$ (kcal/mol)	$-U_{uu}$ (kcal/mol)
Ewald[a]	275	30	SPC/E	11.27 ± 0.03	–	–	–
Reaction Field[b]	270	5	SPC	10.74 ± 0.004	9.950 ± 0.01	0.745 ± 0.002	0.0508 ± 0.002
			SPC/E	10.70 ± 0.004	9.910 ± 0.01	0.763 ± 0.002	0.0529 ± 0.002
Wolf[c]	275	30	SPC/E	11.64 ± 0.04	10.78 ± 0.04	0.730 ± 0.004	0.0568 ± 0.0002
	270	5	SPC	10.62 ± 0.03	9.810 ± 0.01	0.716 ± 0.005	0.0548 ± 0.0002
			SPC/E	11.67 ± 0.03	10.80 ± 0.04	0.734 ± 0.004	0.0568 ± 0.0002

[a] Dornan et al. [95].
[b] Chialvo et al. [20].
[c] This work.

temperature, the magnitude of the AMOEBA and COS/G2 configurational energies are noticeably larger than those obtained from the TIP4P model and the Wolf method, whereas they are appreciably smaller than those calculated by the SPC/E model and the Wolf method. This result is exactly analogous to the result noted formerly by Jiang et al. [114]. Moreover, again at a definite temperature (see Table 4), the AMOEBA and COS/G2 energies are larger than SPC ones using both Lekner and Wolf methods.

It can be seen that in the *NVT* ensemble and at a given temperature, there is almost no difference between the methane–methane internal energies, U_{uu}, which are obtained from the three different water models using the Lekner method. An insignificant difference is also observed between the corresponding water–methane internal energies, U_{wu}, using the Lekner approach. This is caused by the different water potential models, while the methane models are exactly the same. As it is shown in Table 4, these results are reproduced very well by using the Wolf method with each of the three water models. In spite of using the same guest potential models, it can be seen that in the *NPT* data at a given pressure and temperature and for an electrostatic model (see Tables 5 and 6), there is a slight difference between the guest–guest interactions obtained from different water potential models. Such a difference is because of the volume change. However, the dissimilarity between the magnitudes of U_{uu} (and also U_{wu}) calculated from the Wolf method and the analogous results obtained from the Lekner approach is due to the difference between the utilized methane potential models. Furthermore, at 270 K (see Table 4), the negligible discrepancy between the methane–methane and methane–water energies evaluated from the Ewald [27] and Wolf techniques (by considering their uncertainties) is due to the similar rigid methane models (OPLS model) employed in both simulations. A similar finding is attained in *NPT* ensemble simulation for both CH_4 and CO_2 gas hydrates at 270 K and 5 MPa (see Tables 5 and 6), when we compare the guest–guest and guest–host interactions calculated by Wolf method with those obtained from the RF approach.

According to Tables 4–6, in all *NVT* (and *NPT*) data at identical temperatures (and pressures), the SPC water–water energies, U_{ww}, (or even U_{tot}) computed by the Wolf method are reasonably similar to those from other electrostatic models. It is also evident that under the same conditions, the TIP4P water–water interactions (or even U_{tot}) calculated by the Wolf method are equivalent to those obtained from the Lekner technique. However, there are some distinctions between SPC/E water–water energies (or even U_{tot}) evaluated from the Wolf method and the corresponding ones from the RF approach. Therefore, it is necessary to validate the referred energies by comparing them with the data estimated by the other electrostatic models. Considering CH_4 and CO_2 hydrates at 270 K and 30 MPa (see Tables 5 and 6), there is no difference between the SPC/E data evaluated from the Wolf and ES methods. The same result is confirmed in both *NVT* and *NPT* ensembles, when the energies obtained from the Wolf and Lekner methods are compared. Thus under the same conditions, the information computed by the RF method using SPC/E model is slightly different from the corresponding ones obtained from other electrostatic models.

Considering the energies from the Lekner method in both *NPT* and *NVT* ensembles, it is clear that there is a relation between the amounts of the total internal energies calculated from different water potential models, that is, $U_{tot\ (SPC)} < U_{tot\ (TIP4P)} < U_{tot\ (SPC/E)}$. This result is also evident in the present simulation data computed by the Wolf method. It should be mentioned that the relation between the TIP4P and SPC/E energies was pointed out in the study by Jiang et al. [114].

Referring to Tables 5 and 6, for the Wolf method at 270 K and 5 MPa, there are larger host–guest and guest–guest interactions (and consequently larger total interactions) for the CO_2 hydrate than for the methane one, which is due to the larger energy parameter in CO_2 interaction model. This result is equivalent to that given in the study by Chialvo et al. [21]. At 275 K and 30 MPa a similar reason causes a larger U_{tot} for the CO_2 hydrate than for the methane one.

4.2. Radial Distribution Functions (RDFs)

In Figs. 3–6, site–site RDFs of type I CH_4 and CO_2 gas hydrates at 270 K and 5 MPa are displayed, where O indicates water oxygen, H represents hydrogen atom in water and M denotes the center of mass in either guest molecule (CH_4 or CO_2). The RDF is defined as the probability of finding a second molecule at a distance r from a molecule at the origin, relative to the probability expected for a completely random distribution at the same density. The details of the RDF including the definition and formulation are described elsewhere [24,66].

It can be seen that the trends of the host microstructure, i.e., g_{O-O}, g_{O-H} and g_{H-H} in Figs. 3 and 5, show similar characteristics as ambient water [21,72], although higher and narrower correlation peaks appear in the hydrate's host structure [21]. It is evident that all the trends in Figs. 3–6 are similar to those evaluated in the recent *NVT* and *NPT* simulations [21,22,25,26,31,72,114,115]. In addition, all of the three water models produce similar profiles [21,36,72]. However, as was noted by Chialvo et al. [21], there are slightly higher and stronger peaks in the SPC/E trends than in the corresponding SPC ones for both CH_4 and CO_2 gas hydrates. This is because of the larger dipole moment of the water molecule in the SPC/E model (while in both models water molecules have the same geometry).

Figs. 3 and 4 demonstrate that for methane hydrate the first cage separation range is from 3.0 to 5.775 in g_{O-M} and from 4.8 to 9.1 in g_{M-M}. It is also observed that the peak positions in g_{H-M} are only about 0.3 Å less than those in g_{O-M}. These results are close to those reported in the previous simulation studies of the methane hydrate structure [25,72].

The first peak in RDF curve indicates the distribution of the neighboring particles. The first peak in the g_{O-O}, which is about 2.78 Å, corresponds to the nearest interatomic distance between

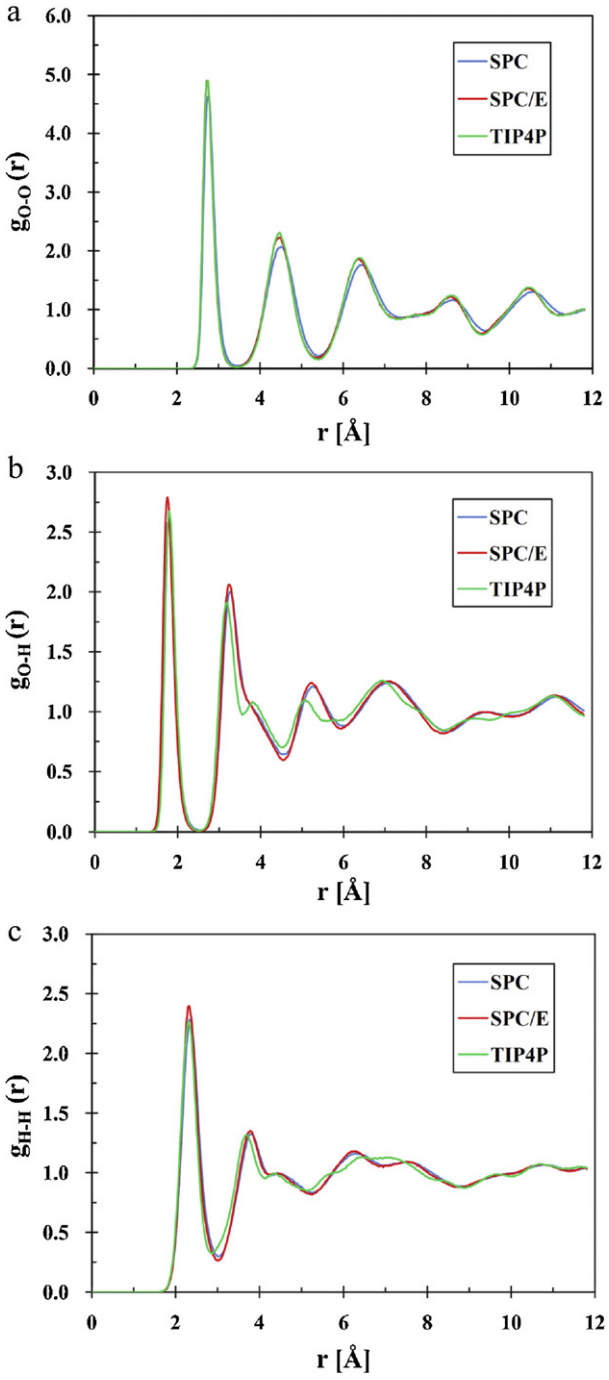

Fig. 3. Water RDFs for the methane hydrate at 270 K and 5 MPa.

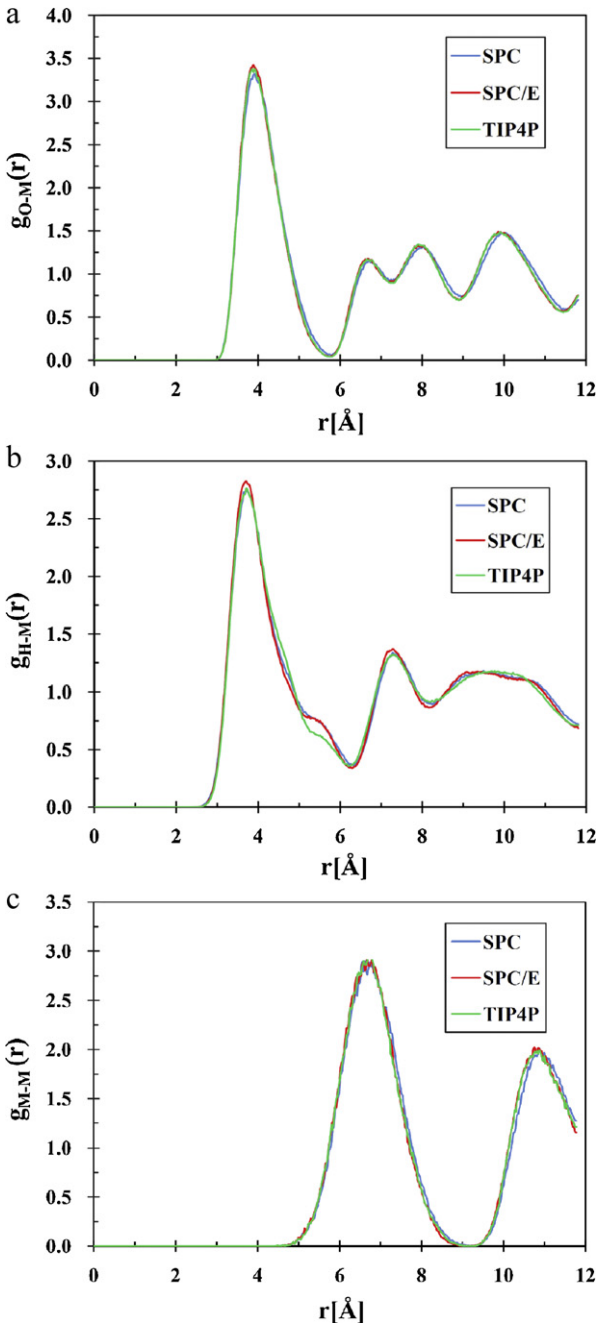

Fig. 4. Guest RDFs for the methane hydrate at 270 K and 5 MPa.

oxygen atoms of the two adjacent water molecules. The second peak appears at a distance about 4.5 Å and indicates the tetrahedrality of the hydrogen bonding [21,22]. The first maximum of g_{O-H}, that is about 1.78 Å, shows the hydrogen bond length in hydrate lattice. This distance is also obtained when the OH bond length in water molecule is subtracted from the nearest oxygen–oxygen distance, i.e., the location of the first peak in g_{O-O}. The first maximal peaks of g_{M-M} and g_{M-O} for methane hydrate occur at 6.62 Å and 3.91 Å, respectively. These quantities are properly consistent to the recent neutron diffraction data and molecular simulation results [4,22,31,66,115]. They are also significantly larger than those observed in methane solution of water [4,115].

In Tables 7 and 8, the locations of the first two peaks of some particle–particle RDFs of CH_4 and CO_2 hydrates evaluated from the present study and some earlier simulations [21,22] are compared. It can be seen that in both simulations the first and second RDF peaks locate in almost similar distances, and hence the present MC

Table 7
Locations of the first two peaks in the RDFs for methane hydrate at 270 K and 5 MPa.

	Location of the first peak (Å)			Location of the second peak (Å)		
	g_{O-O}	g_{O-H}	g_{H-H}	g_{O-O}	g_{O-H}	g_{H-H}
Wolf[a] (MC)	2.775	1.785	2.295	4.515	3.255	3.825
RF[b] (MD)	2.78	1.82	2.3	4.5	3.2	3.8

[a] This work.
[b] Chialvo et al. [20].

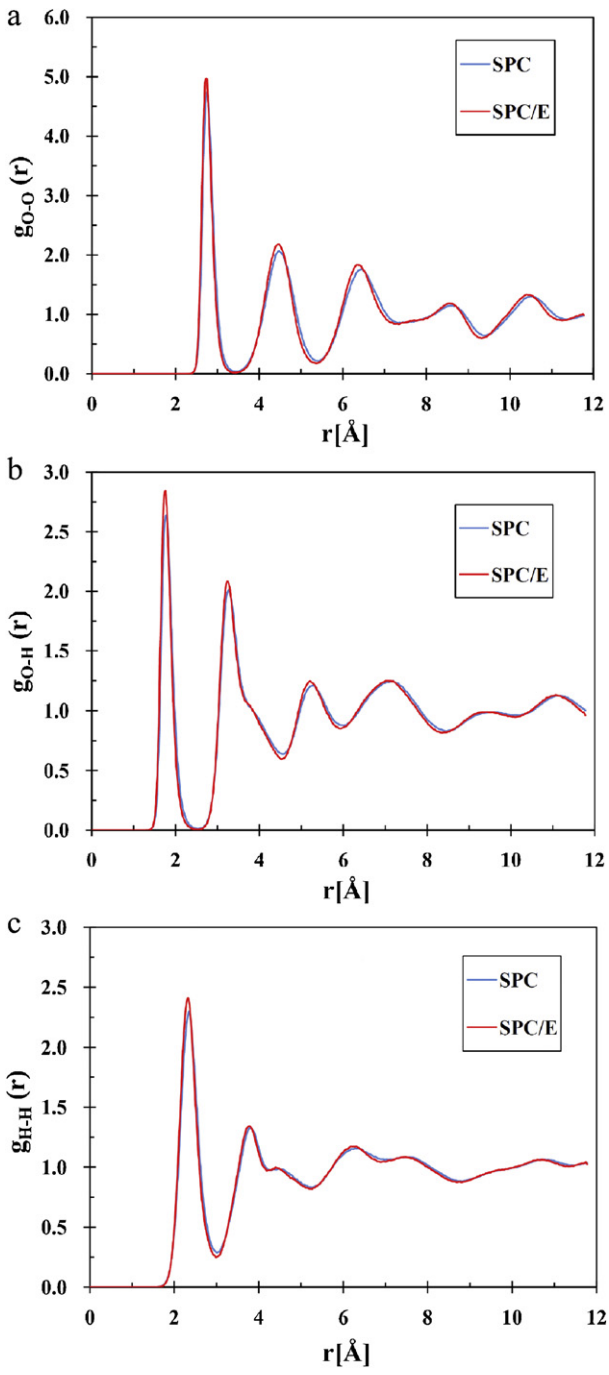

Fig. 5. Water RDFs for the CO_2 hydrate at 270 K and 5 MPa.

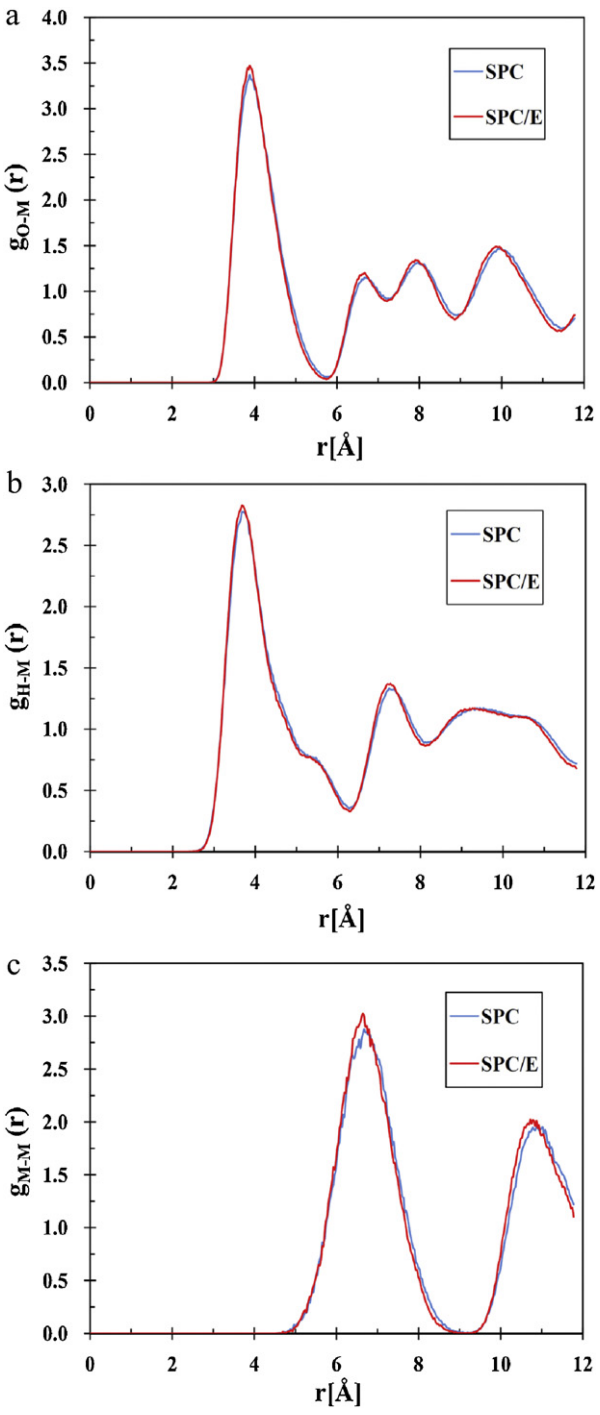

Fig. 6. Guest RDFs for the CO_2 hydrate at 270 K and 5 MPa.

Table 8
Locations of the first two peaks in the RDFs for CO_2 hydrate at 270 K and 5 MPa.

	Location of the first peak (Å)		Location of the second peak (Å)	
	g_{O-O}	g_{M-M}	g_{O-O}	g_{M-M}
Wolf[a] (MC)	2.745	6.675	4.47	10.875
ES[b] (MD)	2.78	6.7	4.53	-[c]

[a] This work.
[b] Geng et al. [21].
[c] Second peak is not given in the paper.

simulation data are in quantitative agreement with the results of the previous Molecular Dynamics (MD) simulations.

5. Conclusion

The Wolf method is proposed to calculate the Coulombic interactions in the simulation of the structure of type I methane and CO_2 clathrate hydrates. The strategy for calculating the necessary parameters α and R_C for this type of hydrates is described and the optimum values are computed. It is demonstrated that the Wolf method is in reasonable agreement with the previous molecular simulation results using Ewald Sum, Reaction Field, and Lekner

methods. In addition, it is shown that in comparison with the ES method and its modifications, the Wolf approach is mathematically simpler and computationally less expensive. It is also more physically justifiable than the ES method for disordered systems, liquids and crystals. In comparison with the RF method, it does not require the dielectric constant, which is unknown in many complex systems and should be evaluated in a self-consistent approach. Considering the computational costs of the Wolf method and the Lekner technique, it can be concluded that the former method is very much faster than the latter one. Given these advantages, the Wolf method seems to be a potential alternate for traditional methods of taking into account the long-range electrostatic interactions in the investigation of the microstructure of more complicated processes such as nucleation and growth in the gas hydrates.

References

[1] J.J. Carroll, Natural Gas Hydrates: A Guide for Engineers, 2nd ed., Gulf Professional Publishing, USA, 2009.
[2] E.D. Sloan, Clathrate hydrates: the other common solid water phase, Industrial Engineering Chemistry Research 39 (2000) 3123–3129.
[3] J. Yoon, M. Chung, H. Lee, Generalized model for predicting phase behavior of clathrate hydrate, AIChE Journal 48 (2002) 1317–1330.
[4] C.A. Koh, R.E. Westacott, W. Zhang, K. Hirachand, J.L. Creek, A.K. Soper, Mechanisms of gas hydrate formation and inhibition, Fluid Phase Equilibria 194–197 (2002) 143–151.
[5] A.H. Mohammadi, R. Anderson, B. Tohidi, Carbon monoxide clathrate hydrates: equilibrium data and thermodynamic modelling, AIChE Journal 51 (2005) 2825–2833.
[6] C.J. Taylor, K.T. Miller, C.A. Koh, E.D. Sloan, Macroscopic investigation of hydrate film growth at the hydrocarbon/water interface, Chemical Engineering Science 62 (2007) 6524–6533.
[7] S. Hashemi, A. Macchi, P. Servio, Gas hydrate growth model in a semibatch stirred tank reactor, Industrial Engineering Chemistry Research 46 (2007) 5907–5912.
[8] J.-W. Jung, J.C. Santamarina, Hydrate formation and growth in pores, Journal of Crystal Growth 345 (2012) 61–68.
[9] E.D. Sloan, C.A. Koh, Clathrate Hydrates of the Natural Gases, 3rd ed., CRC Press, Boca Raton, 2008.
[10] S. Lee, G.D. Holder, Model for gas hydrate equilibria using a variable reference chemical potential: part 1, AIChE Journal 48 (2002) 161–167.
[11] D. Avlonitis, An investigation of gas hydrates formation energetics, AIChE Journal 51 (2005) 1258–1273.
[12] J.W. Tester, R.L. Bivins, C.C. Herrick, Use of Monte Carlo in calculating the thermodynamic properties of water clathrates, AIChE Journal 18 (1972) 1220–1230.
[13] J.S. Tse, W.R. McKinnon, M. Marchi, Thermal expansion of structure I ethylene oxide hydrate, Journal of Physical Chemistry 91 (1987) 4188–4193.
[14] H. Tanaka, Y. Tamai, K. Koga, Large thermal expansivity of clathrate hydrates, Journal of Physical Chemistry B 101 (1997) 6560–6565.
[15] E.M. Freer, M.S. Selim, E.D. Sloan, Methane hydrate film growth kinetics, Fluid Phase Equilibria 185 (2001) 65–75.
[16] R. Sun, Z. Duan, Prediction of CH_4 and CO_2 hydrate phase equilibrium and cage occupancy from ab initio intermolecular potentials, Geochimica et Cosmochimica Acta 69 (2005) 4411–4424.
[17] S. Yoshioki, Application of the independent molecule model to elucidate the dynamics of structure I methane hydrate, Journal of Molecular Graphics and Modelling 25 (2007) 856–869.
[18] Q. Du, D. Li, P. Liu, R. Huang, Molecular potential energies in dodecahedron cell of methane hydrate and dispersion correction for DFT, Journal of Molecular Graphics and Modelling 27 (2008) 140–146.
[19] M.M. Conde, C. Vega, Determining the three-phase coexistence line in methane hydrates using computer simulations, Journal of Chemical Physics 133 (2010) 064507.
[20] S. Liang, P.G. Kusalik, Explorations of gas hydrate crystal growth by molecular simulations, Chemical Physics Letters 494 (2010) 123–133.
[21] A.A. Chialvo, M. Houssa, P.T. Cummings, Molecular dynamics study of the structure and thermophysical properties of model si clathrate hydrates, Journal of Physical Chemistry B 106 (2002) 442–451.
[22] C.Y. Geng, H. Wen, H. Zhou, Molecular simulation of the potential of methane reoccupation during the replacement of methane hydrate by CO_2, Journal of Physical Chemistry A 113 (2009) 5463–5469.
[23] R.J. Sadus, Molecular Simulation of Fluids; Theory, Algorithms and Object Orientation, Elsevier Science, Amesterdam, 2002.
[24] D. Frenkel, B. Smit, Understanding Molecular Simulation, From Algorithms to Applications, Academic Press, San Diego, 2000.
[25] J.S. Tse, M.L. Klein, I.R. McDonald, Molecular dynamics studies of ice IC and the structure I clathrate hydrate of methane, Journal of Physical Chemistry 87 (1983) 4198–4203.
[26] J.S. Tse, M.L. Klein, I.R. McDonald, Computer simulation studies of the structure I clathrate hydrates of methane, tetrafluoromethane, cyclopropane, and ethylene oxide, Journal of Chemical Physics 81 (1984) 6146–6153.
[27] P.M. Rodger, Cavity potential in type I gas hydrates, Journal of Physical Chemistry 93 (1989) 6850–6855.
[28] O.K. Førrisdahl, B. Kvamme, A.D.J. Haymet, Methane clathrate hydrates: melting, supercooling and phase separation from molecular dynamics computer simulations, Molecular Physics 89 (1996) 819–834.
[29] P.L. Chau, R.L. Mancera, Computer simulation of the structural effect of pressure on the hydrophobic hydration of methane, Molecular Physics 96 (1999) 109–122.
[30] E.M. Yezdimer, P.T. Cummings, A.A. Chialvo, Determination of the gibbs free energy of gas replacement in SI clathrate hydrates by molecular simulation, Journal of Physical Chemistry A 106 (2002) 7982–7987.
[31] R.T. Cygan, S. Guggenheim, A.F.K. van Groos, Molecular models for the intercalation of methane hydrate complexes in montmorillonite clay, Journal of Physical Chemistry B 108 (2004) 15141–15149.
[32] V. Chihaia, S. Adams, W.F. Kuhs, Molecular dynamics simulations of properties of a (0 0 1) methane clathrate hydrate surface, Chemical Physics 317 (2005) 208–225.
[33] J. Vatamanu, P.G. Kusalik, Molecular insights into the heterogeneous crystal growth of sI methane H, Journal of Physical Chemistry B 110 (2006) 15896–15904.
[34] G. Tegze, T. Pusztai, G. Tóth, L. Gránásy, A. Svandal, T. Buanes, et al., Multiscale approach to CO_2 hydrate formation in aqueous solution: phase field theory and molecular dynamics. Nucleation and growth, Journal of Chemical Physics 124 (2006) 234710.
[35] B. Kvamme, A. Graue, T. Buanes, T. Kuznetsova, G. Ersland, Storage of CO_2 in natural gas hydrate reservoirs and the effect of hydrate as an extra sealing in cold aquifers, International Journal of Greenhouse Gas Control 1 (2007) 236–246.
[36] L.Y. Ding, C.Y. Geng, Y.H. Zhao, H. Wen, Molecular dynamics simulation on the dissociation process of methane hydrates, Molecular Simulation 33 (2007) 1005–1016.
[37] S. Alavi, K. Udachin, J.A. Ripmeester, Effect of guest–host hydrogen bonding on the structures and properties of clathrate hydrates, Chemistry – A European Journal 16 (2010) 1017–1025.
[38] Y. Iwai, H. Nakamura, Y. Arai, Y. Shimoyama, Analysis of dissociation process for gas hydrates by molecular dynamics simulation, Molecular Simulation 36 (2010) 246–253.
[39] H. Erfan-Niya, H. Modarress, E. Zaminpayma, Molecular dynamics study on the structure I clathrate–hydrate of methane + ethane mixture, Energy Conversion and Management 52 (2011) 523–531.
[40] S. Alavi, R. Ohmura, J.A. Ripmeester, A molecular dynamics study of ethanol–water hydrogen bonding in binary structure I clathrate hydrate with CO_2, Journal of Chemical Physics 134 (2011) 054702.
[41] N.J. English, J.S. Tse, Dynamical properties of hydrogen sulphide motion in its clathrate hydrate from ab initio and classical isobaric–isothermal molecular dynamics, Journal of Physical Chemistry A 115 (2011) 6226–6232.
[42] D. Wolf, P. Keblinski, S.R. Phillpot, J. Eggebrecht, Exact method for the simulation of coulombic systems by spherically truncated, pairwise r^{-1} summation, Journal of Chemical Physics 110 (1999) 8254–8282.
[43] F.N. Mendoza, J. López-Lemus, G.A. Chapela, J. Alejandre, The Wolf method applied to the liquid–vapor interface of water, Journal of Chemical Physics 129 (2008) 024706.
[44] R.J.E. Hockney, Computer Simulation Using Particles, Adam Hilger, Bristol, 1988.
[45] M. Deserno, C. Holm, How to mesh up Ewald Sums. II. An accurate error estimate for the particle–particle–particle-mesh algorithm, Journal of Chemical Physics 109 (1998) 7694–7701.
[46] G.S. Smirnov, V.V. Stegailov, Melting and superheating of sI methane hydrate: molecular dynamics study, Journal of Chemical Physics 136 (2012) 044523.
[47] U. Essmann, L. Perera, M.L. Berkowitz, T. Darden, H. Lee, L.G. Pedersen, A smooth particle mesh Ewald method, Journal of Chemical Physics 103 (1995) 8577–8593.
[48] M.J. Harvey, G.D. Fabritiis, An implementation of the smooth particle mesh Ewald method on GPU hardware, Journal of Chemical Theory and Computation 5 (2009) 2371–2377.
[49] H. Wang, F. Dommert, C. Holm, Optimizing working parameters of the smooth particle mesh Ewald algorithm in terms of accuracy and efficiency, Journal of Chemical Physics 133 (2010) 034117.
[50] T. Darden, D. York, L. Pedersen, Particle mesh Ewald: an N −log(N) method for Ewald sums in large systems, Journal of Chemical Physics 98 (1993) 10089–10092.
[51] M. Deserno, C. Holm, How to mesh up Ewald sums. I. A theoretical and numerical comparison of various particle mesh routines, Journal of Chemical Physics 109 (1998) 7678–7693.
[52] N. Varini, N.J. English, C.R. Trott, Molecular dynamics simulations of clathrate hydrates on specialised hardware platforms, Energies 5 (2012) 3526–3533.
[53] J.A. Greathouse, T.C. Randall, B.A. Simmons, Vibrational spectra of methane clathrate hydrates from molecular dynamics simulation, Journal of Physical Chemistry B 110 (2006) 6428–6431.
[54] C. Moon, P.C. Taylor, P.M. Rodger, Molecular dynamics study of gas hydrate formation, Journal of American Chemical Society 125 (2003) 4706–4707.

[55] A. Demurov, R. Radhakrishnan, B.L. Trout, Computations of diffusivities in ice and CO_2 clathrate hydrates via molecular dynamics and Monte Carlo simulations, Journal of Chemical Physics 116 (2002) 702–709.
[56] J. Zhang, R.W. Hawtin, Y. Yang, E. Nakagava, M. Rivero, S.K. Choi, et al., Molecular dynamics study of methane hydrate formation at a water/methane interface, Journal of Physical Chemistry B 112 (2008) 10608–10618.
[57] J. Vatamanu, P.G. Kusalik, Heterogeneous crystal growth of methane hydrate on its sII [0 0 1] crystallographic face, Journal of Physical Chemistry B 112 (2008) 2399–2404.
[58] S. Liang, P.G. Kusalik, Crystal growth simulations of H_2S hydrate, Journal of Physical Chemistry B 114 (2010) 9563–9571.
[59] Y. Tung, L. Chen, Y. Chen, S. Lin, The growth of structure I methane hydrate from molecular dynamics simulations, Journal of Physical Chemistry B 114 (2010) 10804–10813.
[60] Y. Tung, L. Chen, Y. Chen, S. Lin, Growth of structure I carbon dioxide hydrate from molecular dynamics simulations, Journal of Physical Chemistry C 115 (2011) 7504–7515.
[61] S. Sarupria, P.G. Debenedetti, Molecular dynamics study of carbon dioxide hydrate dissociation, Journal of Physical Chemistry A 115 (2011) 6102–6111.
[62] C.J. Fennell, J.D. Gezelter, Is the Ewald summation still necessary? Pairwise alternatives to the accepted standard for long-range electrostatics, Journal of Chemical Physics 124 (2006) 234104.
[63] P. Demontis, S. Spanu, G.B. Suffritti, Application of the Wolf method for the evaluation of Coulombic interactions to complex condensed matter systems: aluminosilicates and water, Journal of Chemical Physics 114 (2001) 7980–7988.
[64] Y. Ma, S.H. Garofalini, Application of the Wolf damped Coulomb method to simulations of SiC, Journal of Chemical Physics 122 (2005) 094508.
[65] M. Kotelyanskii, D.N. Theodorou, Simulation Methods for Polymers, Marcel Dekker, New York, 2004.
[66] M.P. Allen, D.J. Tildesley, Computer Simulation of Liquids, Clarendon Press, Oxford, 1987.
[67] N. Onsager, Electric moments of molecules in liquids, Journal of American Chemical Society 58 (1936) 1486–1493.
[68] A. Gil-Villegas, S.C. McGrother, G. Jackson, Reaction-field and Ewald summation methods in Monte Carlo simulations of dipolar liquid crystals, Molecular Physics 92 (1997) 723–734.
[69] D. Wolf, Reconstruction of NaCI Surfaces from a dipolar solution to the Madelung problem, Physical Review Letters 68 (1992) 3315–3318.
[70] C. Avendaño, A. Gil-Villegas, Monte Carlo simulations of primitive models for ionic systems using the Wolf method, Molecular Physics 104 (2006) 1475–1486.
[71] A.R. Leach, Molecular Modelling, Principles and Applications, 2nd ed., Prentice Hall, NJ, 2001.
[72] N.J. English, J.M.D. MacElroy, Structural and dynamical properties of methane clathrate hydrates, Journal of Computational Chemistry 24 (2003) 1569–1581.
[73] N.J. English, J.M.D. McElroy, Theoretical studies of the kinetics of methane hydrate crystallization in external electromagnetic fields, Journal of Chemical Physics 120 (2004) 10247–10256.
[74] N.J. English, J.K. Johnson, C.E. Taylor, Molecular-dynamics simulations of methane hydrate dissociation, Journal of Chemical Physics 123 (2005) 244503.
[75] E.J. Rosenbaum, N.J. English, J.K. Johnson, D.W. Shaw, R.P. Warzinski, Thermal conductivity of methane hydrate from experiment and molecular simulation, Journal of Physical Chemistry B 111 (2007) 13194–13205.
[76] L.C. Jacobson, V. Molinero, A methane–water model for coarse-grained simulations of solutions and clathrate hydrates, Journal of Physical Chemistry B 114 (2010) 7302–7311.
[77] J. Lekner, Summation of Coulomb fields in computer-simulated disordered systems, Physica A 176 (1991) 485–498.
[78] A. Bródka, Ewald type summation method for electrostatic interactions in computer simulations of a three-dimensional system periodic in one direction, Chemical Physics Letters 363 (2002) 604–609.
[79] P. Keblinski, J. Eggebrecht, D. Wolf, S.R. Phillpot, Molecular dynamics study of screening in ionic fluids, Journal of Chemical Physics 113 (2000) 282–291.
[80] T.S. Mahadevan, S.H. Garofalini, Dissociative water potential for molecular dynamics simulations, Journal of Physical Chemistry B 111 (2007) 8919–8927.
[81] T.G. Desai, Molecular dynamics study of screening at ionic surfaces, Journal of Chemical Physics 127 (2007) 154707.
[82] D.S. Aidhy, P.C. Millett, T. Desai, D. Wolf, S.R. Phillpot, Kinetically evolving irradiation-induced point defect clusters in UO_2 by molecular dynamics simulation, Physical Review B 80 (2009) 104107.
[83] C. Avendaño, A. Gil-Villegas, E. González-Tovar, Computer simulation of charged hard spherocylinders, Journal of Chemical Physics 128 (2008) 044506.
[84] G. Jiménez-Serratos, C. Avendaño, A. Gil-Villegas, E. González-Tovar, Computer simulation of charged hard spherocylinders at low temperatures, Molecular Physics 109 (2010) 27–36.
[85] E.E. Gdoutos, R. Agrawal, H.D. Espinosa, Comparison of the Ewald and Wolf methods for modeling electrostatic interactions in nanowires, International Journal for Numerical Methods in Engineering 84 (2010) 1541–1551.
[86] R. Agrawal, J.T. Paci, H.D. Espinosa, Large-scale density functional theory investigation of failure modes in ZnO nanowires, Nano Letters 10 (2010) 3432–3438.
[87] A.F. Ghobadi, V. Taghikhani, J.R. Elliott, Investigation on the solubility of SO_2 and CO_2 in imidazolium-based ionic liquids using NPT Monte Carlo simulation, Journal of Physical Chemistry B 115 (2011) 13599–13607.
[88] D. Zahn, B. Schilling, S.M. Kast, Enhancement of the wolf damped coulomb potential: static, dynamic, and dielectric properties of liquid water from molecular simulation, Journal of Physical Chemistry B 106 (2002) 10725–10732.
[89] S.M. Kast, K.F. Schmidt, B. Schilling, Integral equation theory for correcting truncation errors in molecular simulations, Chemical Physics Letters 367 (2003) 398–404.
[90] M.C.C. Ribeiro, Molecular dynamics study on the glass transition in $Ca_{0.4}K_{0.6}(NO3)_{1.4}$, Journal of Physical Chemistry B 107 (2003) 9520–9527.
[91] J.S. Hansen, H. Bruus, B.D. Todd, P.J. Daivis, Rotational and spin viscosities of water: application to nanofluidics, Journal of Chemical Physics 133 (2010) 144906.
[92] G. Kikugawa, R. Apostolov, N. Kamiya, M. Taiji, R. Himeno, H. Nakamura, et al., Application of MDGRAPE-3, a special purpose board for molecular dynamics simulations, to periodic biomolecular systems, Journal of Computational Chemistry 30 (2009) 110–118.
[93] D. Chen, A.C. Stern, B. Space, J.K. Johnson, Atomic charges derived from electrostatic potentials for molecular and periodic systems, Journal of Physical Chemistry A 114 (2010) 10225–10233.
[94] G. Grosso, G.P. Parravicini, Solid State Physics, Academic Press, San Diego, 2000.
[95] P.P. Ewald, Die Berechnung optischer und elektrostatischer Gitterpotentiale, Annalen der Physik 64 (1921) 253–287.
[96] J.W. Perram, H.G. Petersen, S.W. de Leeuw, An algorithm for the simulation of condensed matter which grows as the 3/2 power of the number of particles, Molecular Physics 65 (1988) 875–893.
[97] J. Kolafa, J.W. Perram, Cutoff errors in the Ewald summation formulae for point charge systems, Molecular Simulation 9 (1992) 351–368.
[98] E.L. Pollock, J. Glosli, Comments on P3M, FMM, and the Ewald method for Large Periodic Coulombic Systems, Computer Physics Communications 95 (1996) 93–110.
[99] K. Nam, J. Gao, D.M. York, An efficient linear-scaling Ewald method for long-range electrostatic interactions in combined QM/MM calculations, Journal of Chemical Theory and Computation 1 (2005) 2–13.
[100] Y. Shan, J.L. Klepeis, M.P. Eastwood, R.O. Dror, D.E. Shaw, Gaussian split Ewald: a fast Ewald mesh method for molecular simulation, Journal of Chemical Physics 122 (2005) 054101.
[101] D.S. Cerutti, R.E. Duke, T.A. Darden, T.P. Lybrand, Staggered mesh Ewald: an extension of the smooth particle-mesh Ewald method adding great versatility, Journal of Chemical Theory and Computation 5 (2009) 2322–2338.
[102] N.J. English, D.C. Sorescu, J.K. Johnson, Effects of an external electromagnetic field on rutile TiO_2: a molecular dynamics study, Journal of Physics and Chemistry of Solids 67 (2006) 1399–1409.
[103] N.J. English, Molecular dynamics simulations of liquid water using various long-range electrostatics techniques, Molecular Physics 103 (2005) 1945–1960.
[104] P. Brommer, P. Beck, A. Chatzopoulos, F. Gähler, J. Roth, H. Trebin, Direct Wolf summation of a polarizable force field for silica, Journal of Chemical Physics 132 (2010) 194109.
[105] E. Pantatosaki, G.K. Papadopoulos, On the computation of long-range interactions in fluids under confinement: application to pore systems with various types of spatial periodicity, Journal of Chemical Physics 127 (2007) 164723.
[106] T.J.H. Vlugt, E. Garcia-Perez, D. Dubbeldam, S. Ban, S. Calero, Computing the heat of adsorption using molecular simulations: the effect of strong Coulombic interactions, Journal of Chemical Theory and Computation 4 (2008) 1107–1118.
[107] K.A. Sparks, Configurational properties of water clathrates through molecular simulation, Ph.D. Thesis, Colorado, Massachusetts Institute of Technology, 1991.
[108] R.K. McMullan, G.A. Jeffrey, Polyhedral clathrate hydrates. IX. Structure of ethylene oxide hydrate, Journal of Chemical Physics 42 (1965) 2725–2732.
[109] H.J.C. Berendsen, J.P.M. Postma, W.F. van Gunsteren, J. Hermans, Interaction models for water in relation to protein hydration, in: Intermolecular Forces, Reidel, Dordrecht, 1981, pp. 331–342.
[110] H.J.C. Berendsen, J.R. Grigera, T.P. Straatsma, The missing term in effective pair potentials, Journal of Physical Chemistry 91 (1987) 6269–6271.
[111] W.L. Jorgensen, J. Chandrasekhar, J.D. Madura, R.W. Impey, M.L. Klein, Comparison of simple potential functions for simulating liquid water, Journal of Chemical Physics 79 (1983) 926–935.
[112] P. Dornan, S. Alavi, T.K. Woob, Free energies of carbon dioxide sequestration and methane recovery in clathrate hydrates, Journal of Chemical Physics 127 (2007) 124510.
[113] R. Susilo, S. Alavi, J. Ripmeester, P. Englezos, Tuning methane content in gas hydrates via thermodynamic modeling and molecular dynamics simulation, Fluid Phase Equilibria 263 (2008) 6–17.
[114] H. Jiang, K.D. Jordan, C.E. Taylor, Molecular dynamics simulations of methane hydrate using polarizable force fields, Journal of Physical Chemistry B 111 (2007) 6486–6492.
[115] C.A. Koh, R.P. Wisbey, X. Wu, R.E. Westacott, A.K. Soper, Water ordering around methane during hydrate formation, Journal of Chemical Physics 113 (2000) 6390–6397.